NAC-0053_R0

Safety Evaluation Report Response

25 November 2015

Prepared for Energy*Solutions* by
NEPTUNE AND COMPANY, INC.
1435 Garrison St, Suite 110, Lakewood, CO 80215

1. Title: Safety Evaluation Report Response		
2. Filename: SER Response.docx		
3. Description: Response to Utah Dept. of Environmental Quality, Division of Waste Management and Radiation Control, Safety Evaluation Report (SC&A 2015).		
	Name	Date
4. Originator	Mike Sully	15 September 2015
5. Reviewer	Kate Catlett, Paul Black	25 November 2015
6. Remarks		

CONTENTS

FIGURES

TABLES

ACRONYMS AND ABBREVIATIONS

DEQ	Utah Department of Environmental Quality
DRC	Division of Radiation Control
DU	depleted uranium
DWMRC	Division of Waste Management and Radiation Control
ES	Energy*Solutions*
NRC	U.S. Nuclear Regulatory Commission
PA	performance assessment
SER	safety evaluation report

1.0 Introduction

Based on its review of Round 3 Interrogatories, the Utah Department of Environmental Quality (DEQ) had additional questions regarding the performance of the evapotranspiration (ET) cover system and deep time modeling as part of the Clive Depleted Uranium (DU) Performance Assessment (PA) Model (the Clive DU PA Model) constructed by Neptune and Company, Inc. (Neptune). These concerns were discussed with Energy*Solutions* (ES) and, on August 11, 2014, DEQ submitted additional interrogatories for ES to address. DEQ also requested that ES conduct some additional bounding calculations with HYDRUS to provide greater transparency as to how the percolation model performed. ES' replies are documented in its August 18, 2014, "Responses to August 11, 2014 – Supplemental Interrogatories Utah LLRW Disposal License RML UT 2300249 Condition 35 Compliance Report".

DEQ reviewed the responses in ES (2014) and determined that the information provided was not sufficient to resolve the supplemental interrogatories. Their review is documented in the Safety Evaluation Report (SER) (SC&A 2015, Volume 2, Appendix B). In general, DEQ decided that there needs to be much more description of how the analysis proceeded from the input data to the results. Appendix B of SC&A (2015, Volume 2) includes specific examples from the ES response where DEQ believes that additional information and explanations are necessary.

This document provides the additional information and explanation requested by DEQ. Note that DEQ and DRC (Division of Radiation Control) are used interchangeably within this document. In addition, in July 2015, the DRC was merged with another division and renamed the Division of Waste Management and Radiation Control (DWMRC). Furthermore, the SER was prepared by SC&A, Inc., so references to the SER are cited as "SC&A, 2015".

2.0 Evapotranspiration and Infiltration

This section provides an alternative net infiltration and volumetric water content model for the Clive DU PA Model v1.4 that represents a cover system with different hydraulic properties and clearly correlates the hydraulic parameters alpha and hydraulic conductivity. This alterative model is named the "v1.4XXX Benson" model. The flow models used were developed to account for changes in hydraulic properties due to plant and animal activity and frost action that might affect the net infiltration rate and water content status based on the conceptual model of cover "naturalization" described in the work of Benson et al. (2011) and in Appendix E of SC&A (2015), Volume 2. This approach to modeling of flow takes into account changes in hydraulic properties due to biological activity and freeze/thaw cycles predicted by the conceptual model of cover naturalization.

For this set of unsaturated zone flow models, the cover system is considered to be entirely homogeneous with respect to hydraulic properties other than a minor adjustment to a parameter (gravel adjustment) for the surface layer. Input parameters for these infiltration models are derived from the distributions and methods described by Dr. Craig Benson in Volume 2, Appendix E, of the safety evaluation report (SER) prepared by SC&A (SC&A 2015), consistent with the request of DEQ to use this approach (SC&A 2015).

These models represent modifications to previous models required in response to the SER issues. These models are conservative and do not represent the likely evolution of the cover system Differences between the homogenous cap and the Clive DU PA Model v1.4 conceptual models are described in the discussion following the model results.

2.1 Methods

The evapotranspiration (ET) cover design, unsaturated zone and shallow aquifer characteristics, climate, and vegetation are described in detail in Appendix 5 of the Final Report for the Clive DU PA Model v1.4. The infiltration models include 50 HYDRUS-1D (H1D) simulations using homogeneous properties (except for the gravel correction in the surface layer) and the method for developing hydraulic property values provided in Appendix E of the SER (SC&A 2015). H1D was used to estimate water contents with depth in the ET cover, and to estimate average annual drainage out of the bottom of the cover into the waste zone (net infiltration). Simulation durations were 1,000 years. Mean water contents and infiltration rates for each parameter set were calculated from the last 100 years of the 1,000-year simulations.

For the homogenized cap model, the following changes were made from previous ET cover simulations:

- Deeper rooting depth (1.5 m), with constant root density throughout the 1.5-m cover profile
- Homogenous hydraulic properties (except for gravel correction of saturated water content in surface layer).

Figure 1 illustrates the homogeneous material distribution, constant root density, and locations of observation nodes used for the naturalized H1D model.

2.2 Surface Boundary Conditions

The WGEN model (Richardson and Wright 1984) was used to generate a 100-year synthetic daily record of precipitation, maximum temperature, and minimum temperature for the site. Use of the WGEN model, a component of the HELP model (Schroeder et al. 1994a; Schroeder et al. 1994b), is consistent with U.S. NRC guidance (Meyer et al. 1996). The 100-year record was generated using the monthly average values from measurements at the site based on 17 years of observations. Simulations were run for 1,000 years repeating the 100-year daily boundary conditions. The model is deliberately run for a long period of time (1,000 years) in order to reach a near-steady state net infiltration rate that is not influenced by the initial conditions. Long-term variations in climate are addressed in the Deep Time Model.

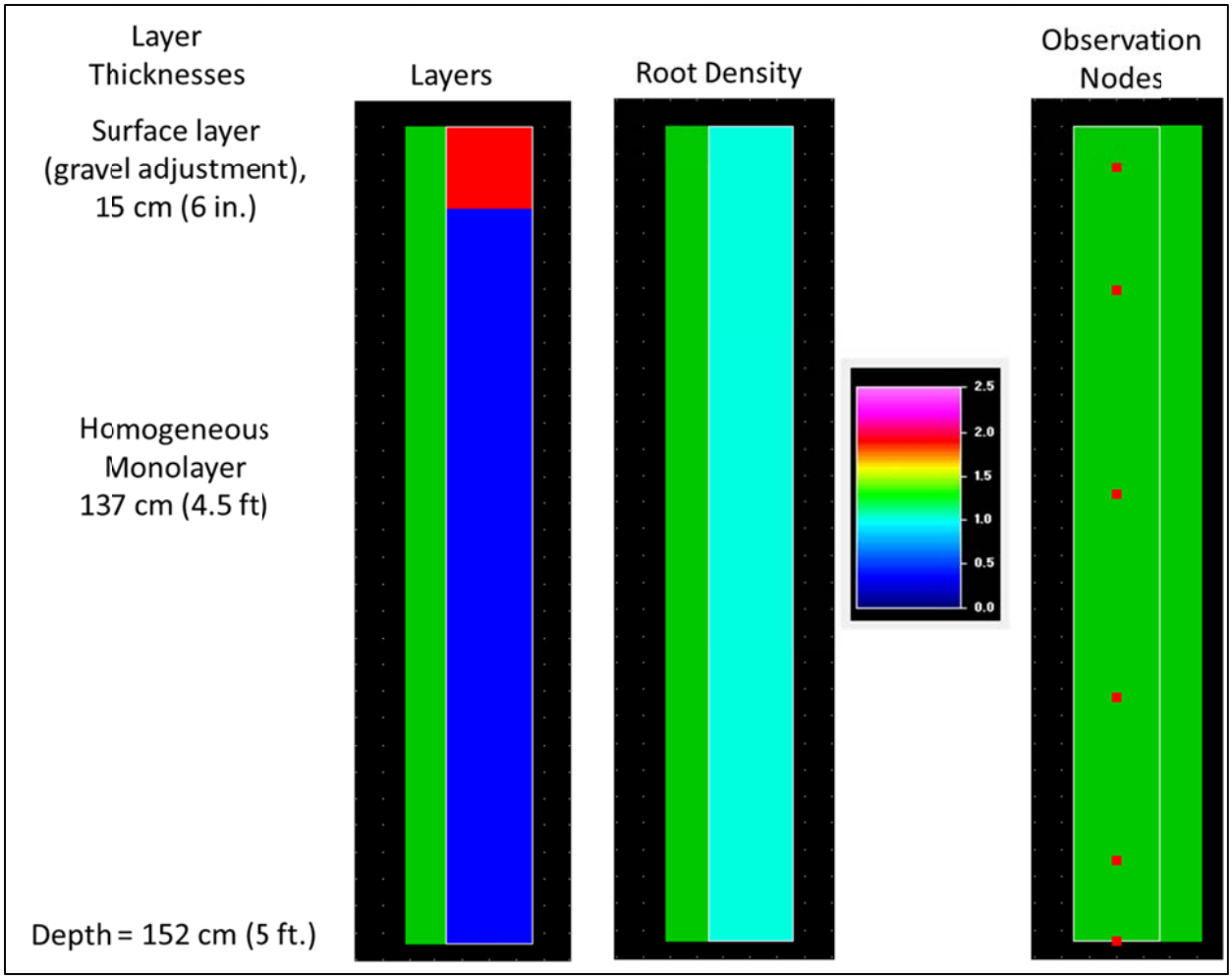

Figure 1. Model layers, root density, and observation nodes for naturalized H1D model.

2.3 Hydraulic Properties

Hydraulic property values for these simulations were generated using the method described by Benson in Appendix E, Volume 2, of SC&A (2015). Using the EXCEL spreadsheet provided, "Hyd Props Calculator.xls," 50 combinations of the alpha, n, saturated water content (theta_s), and saturated hydraulic conductivity (Ks) were generated. For the 50 combinations of parameters, the generated Ks and alpha values were correlated using a correlation coefficient of 0.48 provided in SC&A (2015). Recommended standard deviations for the four parameters were chosen from the "Low" column of Table 2 in Appendix E (SC&A 2015), shown in Table 1 below, to keep the input parameters within the ranges recommended in Benson et al. (2011). No additional upscaling of the parameter values was done for these parameter sets. The 50 parameter sets used for the models are shown in Table 2 below. The parameter theta_s* corresponds to the generated value of the saturated water content corrected for the addition of gravel in the surface layer.

Table 1. Recommended mean values and standard deviations for hydraulic parameters from Appendix E of SC&A (2015).

Parameter	Base Units	Mean	Standard Deviation
lnKs	m/s	-14.51	0.59
lnalpha	1/kPa	-1.609	0.12
n	-	1.3	0.04
theta_s	-	0.4	0.013

Table 2. Hydraulic parameter sets generated using "Hyd Props Calculator.xls" as described in Appendix E of SC&A (2015).

Realization	theta_s*	theta_s	alpha (1/cm)	n	Ks (cm/d)
1	0.331	0.389	0.0255	1.24	15.49
2	0.358	0.421	0.0184	1.29	12.08
3	0.323	0.380	0.0216	1.39	9.77
4	0.345	0.406	0.0230	1.37	10.09
5	0.339	0.399	0.0195	1.31	4.42
6	0.347	0.409	0.0209	1.32	2.38
7	0.352	0.414	0.0177	1.28	2.11
8	0.349	0.411	0.0254	1.29	3.64
9	0.333	0.392	0.0191	1.36	6.00
10	0.341	0.401	0.0203	1.39	3.45
11	0.345	0.405	0.0175	1.31	3.22
12	0.343	0.403	0.0218	1.32	4.89
13	0.336	0.396	0.0187	1.29	2.48
14	0.345	0.405	0.0241	1.30	7.31
15	0.348	0.410	0.0201	1.24	6.70
16	0.346	0.407	0.0149	1.27	1.59
17	0.330	0.388	0.0185	1.32	3.55
18	0.339	0.399	0.0184	1.33	1.10
19	0.342	0.402	0.0204	1.29	12.83
20	0.340	0.401	0.0212	1.30	2.85
21	0.361	0.425	0.0179	1.20	4.76
22	0.342	0.402	0.0244	1.27	4.15
23	0.345	0.406	0.0193	1.34	3.89
24	0.335	0.394	0.0205	1.33	3.94
25	0.325	0.382	0.0171	1.30	1.39
26	0.336	0.396	0.0220	1.30	5.59
27	0.340	0.400	0.0190	1.25	5.22
28	0.338	0.398	0.0245	1.28	9.18
29	0.353	0.416	0.0173	1.33	2.76
30	0.340	0.400	0.0152	1.19	2.22
31	0.343	0.403	0.0183	1.31	1.94
32	0.332	0.390	0.0195	1.31	2.00
33	0.308	0.362	0.0199	1.27	5.75
34	0.334	0.393	0.0214	1.28	3.31
35	0.337	0.397	0.0183	1.35	3.08
36	0.336	0.395	0.0241	1.23	4.71
37	0.349	0.411	0.0197	1.31	8.69
38	0.325	0.382	0.0206	1.31	4.47
39	0.331	0.389	0.0178	1.27	4.20
40	0.328	0.386	0.0222	1.28	6.48

Realization	theta_s*	theta_s	alpha (1/cm)	n	Ks (cm/d)
41	0.355	0.418	0.0192	1.22	3.41
42	0.355	0.418	0.0227	1.33	3.46
43	0.341	0.401	0.0172	1.33	3.50
44	0.335	0.394	0.0241	1.29	11.49
45	0.343	0.403	0.0186	1.30	4.96
46	0.346	0.407	0.0213	1.24	4.65
47	0.345	0.405	0.0200	1.27	7.47
48	0.327	0.384	0.0194	1.32	2.33
49	0.337	0.397	0.0178	1.33	6.93
50	0.340	0.401	0.0209	1.29	6.38

2.4 HYDRUS Simulation Results

Net infiltration for each of the 50 replicate input parameter sets is plotted in Figure 2 below. Net infiltration ranged from 0.57 mm/yr to 1.31 mm/yr with a mean value of 0.91 mm/yr. Results for volumetric water content and net infiltration for each realization are provided in Appendix A.

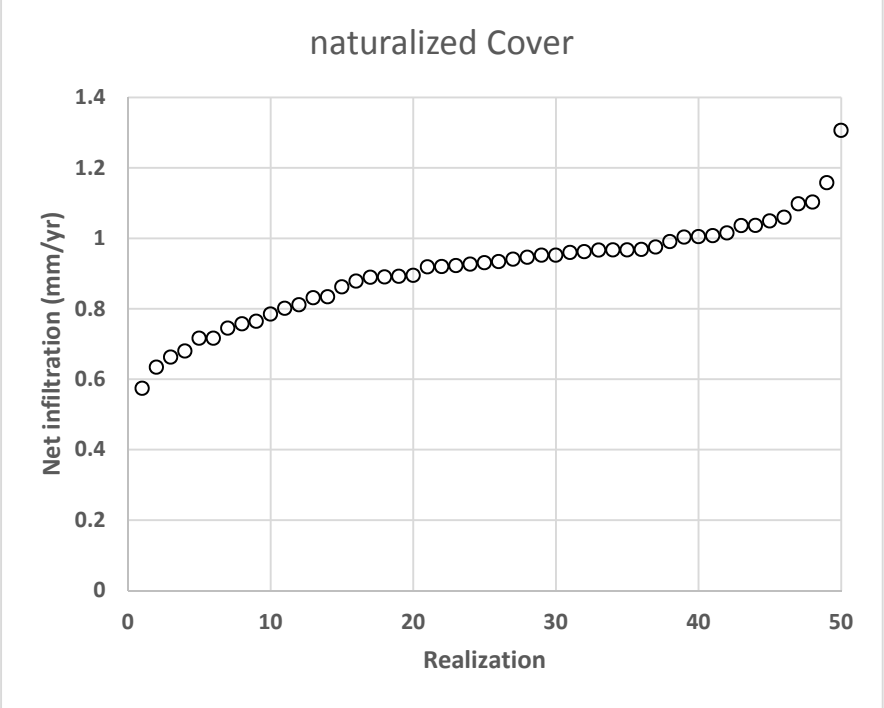

Figure 2. Net infiltration rate estimated by HYDRUS-1D for 50 combinations of hydraulic properties generated using the method described by Benson in Appendix E, Volume 2, of SC&A (2015).

2.4.1 Water Balance Results

Five of the 50 naturalized cover simulations were selected for summarizing the water balances. The five selected are realizations #41, 7, 25, 20, and 24 of the 50 simulations, which correspond

to the 10th, 30th, 50th, 70th and 90th percentile infiltration values, respectively. Net infiltration rates for the water balance analyses ranged from 0.711 mm/yr to 1.038 mm/yr. The major components of the water balance for the five simulations are shown in Figure 3 below.

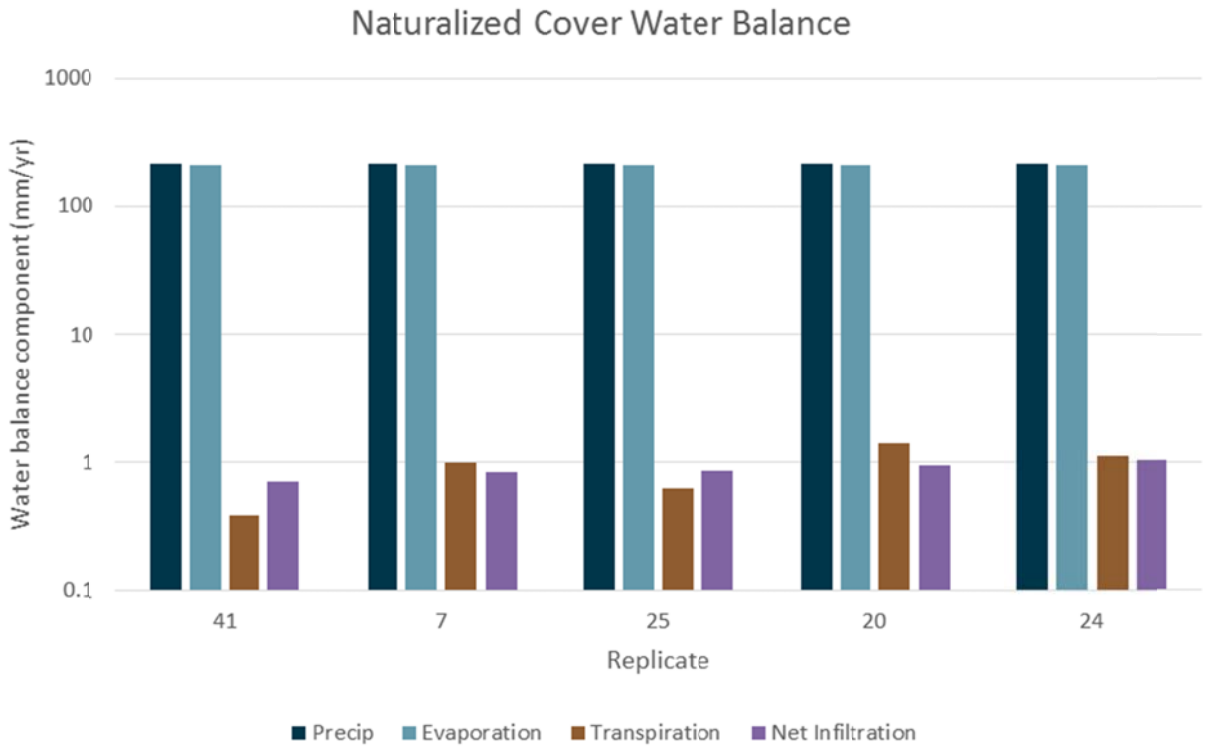

Figure 3. Water balance components for naturalized cover simulations in order of increasing net infiltration.

Table 3 summarizes the water balance components from the five simulations in more detail. Total water balance errors for the five simulations are on average about 0.56 mm/yr or 0.27 percent of the total annual precipitation.

Changes in storage are zero when averaged over the last 100 years of the simulations. Runoff is also negligible. The water balance plots in Figure 3 show the remaining components of water balance: precipitation, evaporation, transpiration, and net infiltration.

Table 3. Water balance components for five of the 50 homogeneous cover hydraulic property simulations.

	Replicate 41		Replicate 7		Replicate 25		Replicate 20		Replicate 24	
Water Balance Component	mm/yr	% of Precip	mm/yr	% of Precip	mm/yr	% of Precip	mm/yr	% of Precip	mm/yr	% of Precip
Precipitation	212.3		212.0		212.3		212.0		212.1	
Evaporation	210.6	99.20	209.7	98.92	210.1	98.96	209.1	98.63	209.4	98.73
Transpiration	0.389	0.18	0.982	0.46	0.625	0.29	1.444	0.68	1.127	0.53
Net Infiltration	0.711	0.34	0.848	0.40	0.865	0.41	0.955	0.45	1.038	0.49
Runoff	1.56 E-04	0.00	1.37 E-04	0.00	1.36 E-04	0.00	1.02 E-04	0.00	9.75 E-05	0.00
Storage	0.00	0.00	0.00	0.00	0.00	0.00	0.00	0.00	0.00	0.00
Total	211.7	99.72	211.5	99.78	211.6	99.67	211.5	99.76	211.6	99.75
Mass balance error	0.599	0.28	0.470	0.22	0.710	0.33	0.501	0.24	0.535	0.25

2.5 Regression Model Development

2.5.1 Exploratory Data Plots

Exploratory scatter plots for each depth zone showed generally linear relationships between the covariates alpha, n, Ks, and theta_s and the response variables water content and net infiltration flux model results. The saturated water content of the surface layer (theta_s*) was not included as a parameter in the linear regression since it is derived from adjusting the value of theta_s. These relationships are shown in Figure 7 through Figure 12 in Appendix B for zones in the naturalized cover corresponding to depths of the surface (WC1), evaporative (WC2), frost protection (WC3), upper radon barrier (WC4), and lower radon barrier (WC5) layers for water content and the net infiltration at the top of the waste.

2.5.2 Linear Regression Models

Multiple linear regression models were fit to the HYDRUS simulations for each layer. The general form of the regression was:

$$Y = \beta_0 + \beta_1 * Ks + \beta_2 * alpha + \beta_3 * n + \beta_4 * theta\_s$$

Net infiltration was converted to units of cm/day and volumetric water content was dimensionless. The regressions were fit using the "`lm()`" function in the software package *R*, which uses least squares for estimating parameters.

The statistics underlying linear regression assume that the coefficients are distributed as normal, so the coefficient estimates and their associated standard error estimates represent the mean and

standard deviation from a normal distribution. Regression coefficients are shown in Table 4 below.

Table 4. Fitted model coefficients.

Response	β_0	β_1	β_2	β_3	β_4
Surface WC	0.37326	-0.00309	-0.19961	-0.26633	0.32691
Evap WC	0.45616	-0.00365	-0.27057	-0.32052	0.39271
Frost WC	0.47409	-0.00341	-0.38131	-0.33119	0.38654
Rn1 WC	0.48466	-0.00325	-0.45964	-0.33817	0.38318
Rn2 WC	0.48888	-0.00319	-0.49211	-0.34102	0.38190
Flux	-0.00029	-3.5389E-6	0.00574	0.00065	-0.00100

2.6 Implementation in GoldSim

The following changes are made to the Clive Model v1.4; the resulting model iteration is referred to as v1.4XXX Benson.

Using Table 4, the resulting equations for infiltration and water content in GoldSim become:

$$Infil = \beta_0 + \beta_1 * Ks + \beta_2 * alpha + \beta_3 * n + \beta_4 * theta\_s$$

$$WC = \beta_{i,0} + \beta_{i,1} * Ks + \beta_{i,2} * alpha + \beta_{i,3} * n + \beta_{i,4} * theta\_s$$

where Infil is net infiltration in cm/day, WC is the average volumetric water content, and β values are the linear regression coefficients with the subscript i corresponding to Surface, Evaporative, Frost protection, Upper radon barrier, and Lower radon barrier depth zones listed in Table 4.

After the water content is calculated, GoldSim expression elements are used to enforce physical bounds of water content as the residual water content (if the water content is less than the residual water content) and as the porosity (if water content is greater than porosity).

The input parameters Ks, alpha, n, and theta_s for each realization are obtained from a lookup table of 1000 realizations generated using the method described by Benson in Appendix E, Volume 2 of SC&A (2015). A lookup table is used for the inputs rather than stochastic elements in GoldSim to force a correlation between ln alpha and ln Ks since GoldSim does not include a multivariate normal distribution for representing correlation.

2.7 Results

Results of this simulation are compared to those of the Clive DU PA Model v1.4 in Table 5 and Table 6.

Groundwater concentrations of Tc-99 and Rancher doses are compared in Table 5. The greater infiltration of the homogenized cap leads to higher groundwater concentrations. The Tc-99 median concentration is below the groundwater protection limit (GWPL) of 3790 pCi/L, while the mean and 95th percentile results exceed the GWPL. Rancher doses are slightly lower in the v1.4XXX Benson model because the increased infiltration suppresses upward radon flux.

Table 5. Groundwater and ranch dose results for v1.4XXX Benson compared to v1.4.

	Mean		Median		95th Percentile	
	v1.4*	v1.4XXX Benson	v1.4*	v1.4XXX Benson	v1.4*	v1.4XXX Benson
Peak Tc-99 groundwater concentration within 500 yr (pCi/L)	2.6E1	7.6E3	4.3E-2	3.0E2	1.5E2	4.1E4
Peak rancher dose within 10,000 yr (mrem/yr)	6.2E-2	5.1E-2	5.1E-2	4.5E-2	1.5E-1	1.2E-1
* v1.4 results are based on 10,000 realizations, while other results in this table are based on 1,000 realizations.						

Deep time results are compared in Table 6. The homogenized cap model produces lower lake and sediment concentrations because increased infiltration suppresses upward diffusion of radionuclides in the model.

Table 6. Comparison of deep time results at model year 90,000 for v1.4XXX Benson with v1.4. All results based on 1000 realizations.

	25th Percentile		Median		Mean		95th Percentile	
	v1.4	v1.4XXX Benson	v1.4	v1.4XXX Benson	v1.4	v1.4XXX Benson	v1.4	v1.4XXX Benson
U-238 lake concentration (pCi/L)	1.4E-7	1.4E-7	2.1E-5	1.3E-5	1.8E-2	3.9E-3	1.1E-1	1.5E-2
Ra-226 lake concentration (pCi/L)	8.5E-3	2.0E-4	1.5E-1	9.4E-3	5.4E-1	6.2E-2	2.4E0	3.0E-1
U-238 sediment concentration (pCi/g)	1.7E-4	1.3E-7	1.8E-3	5.3E-6	2.0E-2	2.4E-4	9.5E-2	1.1E-3
Ra-226 sediment concentration (pCi/g)	6.9E-5	1.7E-6	1.2E-3	7.1E-5	5.0E-3	5.8E-4	2.2E-2	2.9E-3

2.8 Sensitivity Analysis of GoldSim v1.4XXX Benson

A sensitivity analysis of the ^{99}Tc groundwater concentrations with 500 years and rancher doses within 10,000 years was performed in order to determine which modeling parameters are most significant in predicting these results. The most sensitive parameters for these endpoints are presented in Table 3.

The soil-water partition coefficient (K_d) was the most sensitive parameter for the groundwater concentration of ^{99}Tc. K_d controls sorption to the solid phase, with higher K_d resulting in increased sorption which retards migration of the radionuclides. In model version 1.4, the most sensitive parameter for groundwater concentrations of ^{99}Tc was van Genuchten's α, which is involved in the water content and infiltration regression equations. In v1.4XXX Benson, the homogenized cover leads to much high infiltration rates, and the model is thus not as sensitive to the regression inputs compared to v1.4.

The most sensitive input parameter for rancher dose is the radon E/P ratio, which defines the fraction of ^{222}Rn that escapes into the mobile environment when formed by radioactive decay from its parent, ^{226}Ra. Radon that does not escape but remains within the matrix of the radium-containing waste material stays in place and decays to polonium and then to ^{210}Pb. Note that the higher the E/P ratio, the higher the dose.

Table 7. Sensitive input parameters for v1.4XXX Benson.

	SI rank	Input parameter	Sensitivity index (SI)
Peak ^{99}Tc groundwater concentration within 500 years	1	K_d for Tc [1]	43
	2	Activity Concentration of Tc-99 in SRS DU Waste	16
	3	Molecular Diffusivity in Water	14
	4	Van Genuchten's n	5
Peak rancher dose within 10,000 years	1	Radon Escape/Production Ratio for Waste	38
	2	K_d for Ra in sand	3.61

[1] For technetium, the same K_d value was used for all materials.

2.9 Discussion

The hydraulic property recommendations and cover material naturalization present in Benson et al. (2011) and in Appendix E (SC&A, 2015) are inappropriate for the Clive site. When included in the model, they produce a model that does not make sense for the site conditions of Clive. This model can be considered "conservative" in terms of modeling groundwater concentrations

but dose results are lower for this model implementation than for the Clive DU PA Model v1.4, which does not imply "conservative." The rationale for not using these homogenized cap properties in the Clive DU PA Model v1.4 are presented in this section.

The hydraulic property recommendations provided in Benson et al. (2011) are based on measurements for samples from in-service covers made at 12 sites throughout the continental United States. One element of the characterization of a site's climate is the ratio of mean annual precipitation to mean annual potential evapotranspiration. The magnitude of this ratio is estimated to be 0.17 for Clive. Only one of the sites sampled by Benson et al. (2011) was considered to be arid, having a ratio of 0.06. The mean value of this ratio for all sites sampled was 0.51, with a highest value of 1.10. At two of the sites rainfall exceeded potential evaporation, which is completely inappropriate for the arid conditions at Clive. All but one of the sites that form the basis for the hydraulic property recommendations have much wetter conditions than Clive.

The conceptual model of cover material "naturalization" for Clive based on the work of Benson et al. (2011) is described in Appendix E of SC&A (2015) as including changes in the hydraulic behavior of the material following construction. These changes are characterized by increasing values of hydraulic properties such as Ks and the hydraulic function alpha parameter that begin soon after cover completion. These changes are commonly attributed to pedogenic processes including wet-dry and freeze-thaw cycles, activity of roots and soil animals, decomposition of organic matter by microbes producing compounds that tend to bind soil particles into aggregates, and changes in cations adsorbed onto soil particle surfaces. In this conceptual model these processes lead to the development of soil structure but not soil horizons.

Under the wetter conditions considered by Benson et al. (2011), plant and animal activity are greater than in an arid setting. These wetter conditions promote a faster rate of disruptive processes due to plant and animal activity and in some cases freeze-thaw activity that were shown by Benson et al. (2011) to lead to formation of an aggregated soil structure and natural mixing of soil layers at their study sites. Most importantly, the sites considered by Benson et al. (2011) also lack significant eolian deposition. This is not the case for a site like Clive. Recent field studies (Neptune 2015) provide evidence for a site-specific conceptual model of weak development of soil profiles (limited pedogenesis) in a setting influenced by low rates of deposition of eolian silt in the Holocene history. The Site is within a region of significant eolian activity evidenced by locally thick accumulation of gypsum dunes west and southwest of the site and a laterally continuous layer of suspension fallout silts preserved beneath the modern surface throughout the Clive site. Clive quarry exposures examined in a field study (Neptune 2015) showed sections of eolian silts immediately below a modern vegetated surface (Figure 4). The bottom of the eolian silt formed a gradational but definable contact with the lake muds and marl below. The upper vegetated surface at the top of the eolian section was distinct and noted as being partially indurated. In addition, buried soils were found in the eolian and lake sediments below the Lake Bonneville lacustrine sequence.

The eolian deposits in the upper part of the stratigraphic section shown in Figure 4 represent a 10,000-year-old record of deposition and soil formation (Neptune 2015). Primary soil features developed over this time interval include an indurated Av-zone, and slight reddening of the silt profile with local platy structure from formation of clays (Figure 5). These observations are

consistent with slow processes of pedogenesis in a high elevation semi-arid setting and continuing suppression and burial of developing soils by a relatively low rate of deposition of eolian silt. There is no evidence of soil structure development extensive enough to influence soil hydraulic properties.

Observations of Holocene eolian silt throughout the Clive site support a conceptual model of long-term eolian deposition on a stable surface that promotes and preserves concurrent eolian deposits which are only slightly modified by slow processes of soil formation. The past Holocene depositional conditions at the Clive site are promoted by a combination of extensive wet playa sources of eolian source material to the west and southwest of the Clive site and the extremely low gradient paleo-Lake Bonneville surface surrounding the site with sparse surface vegetation and limited surface erosion. These conditions will persist at the Clive site as long as the lake levels remain below the site elevation. Rates of eolian deposition would be expected to increase as future lakes approach the site with increased formation of dunes (deposition of eolian sands). Recurring lakes during ice ages (climate cycles) will rework and mix the eolian deposits with aggrading clastic lake sediments. The expectation is that eolian deposits will drape and slightly stabilize closure covers until future lakes return to the Clive site.

Climate conditions and soil formation processes at the Clive site contradict the assumptions of the homogenized cap and demonstrate the inapplicability of the homogenized cap to the Clive site.

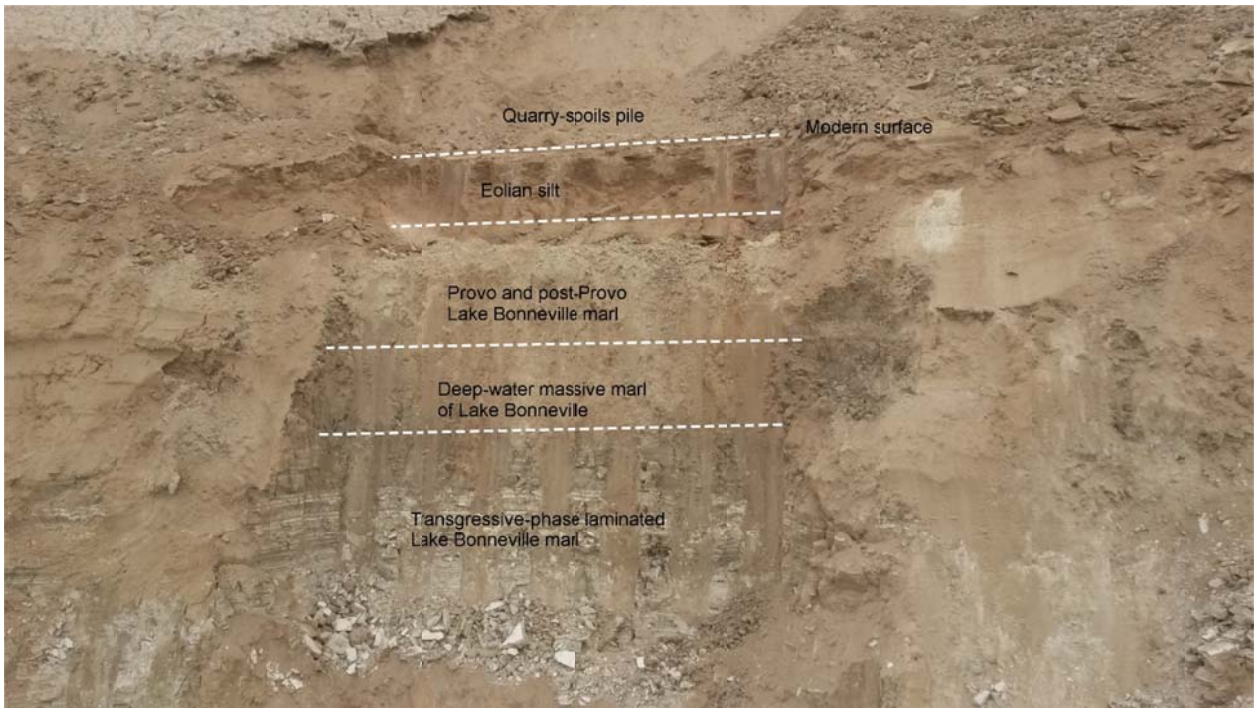

Figure 4. Eolian silt in trench located at Clive Pit 29 overlying Lake Bonneville sedimentary deposits (Neptune 2015).

Figure 5. An example of upper soil-modified eolian silt in Pit 29. Basal contact of the silt is approximately located at the middle of the pick handle. It is a gradational contact between eolian silt intermixed with regressive Lake Bonneville marl (bottom of the pick handle).

3.0 GoldSim Quality Assurance — Comparison with GoldSim Results

This section provides a comparison between two sets of net infiltration rates, one calculated directly from the HYDRUS models and the other from linear models abstracted from the HYDRUS results. The first set consists of net infiltration rates obtained from the 50 HYDRUS simulations using naturalized material properties and correlated values of ln Ks and ln alpha. The second set consists of 1,000 realizations of net infiltration from the GoldSim Model (v1.4XXX Benson). These were calculated using the linear model with coefficients from Table 4 for net infiltration, and input parameter values for Ks, alpha, n, and theta_s from a lookup table of 1,000 parameter sets generated using the method described by Benson in Appendix E, Volume 2, of SC&A (2015).

The HYDRUS and linear model net infiltration rates are compared in Figure 6. These results match closely, assuring consistency in the results of these two models. Net infiltration from the HYDRUS simulations ranged from 0.57 mm/yr to 1.31 mm/yr with a mean value of 0.91 mm/yr. Net infiltration calculated from the linear model used in the GoldSim v.1.3 Model coefficients ranged from 0.57 mm/yr to 1.29 mm/yr with a mean of 0.93 mm/yr.

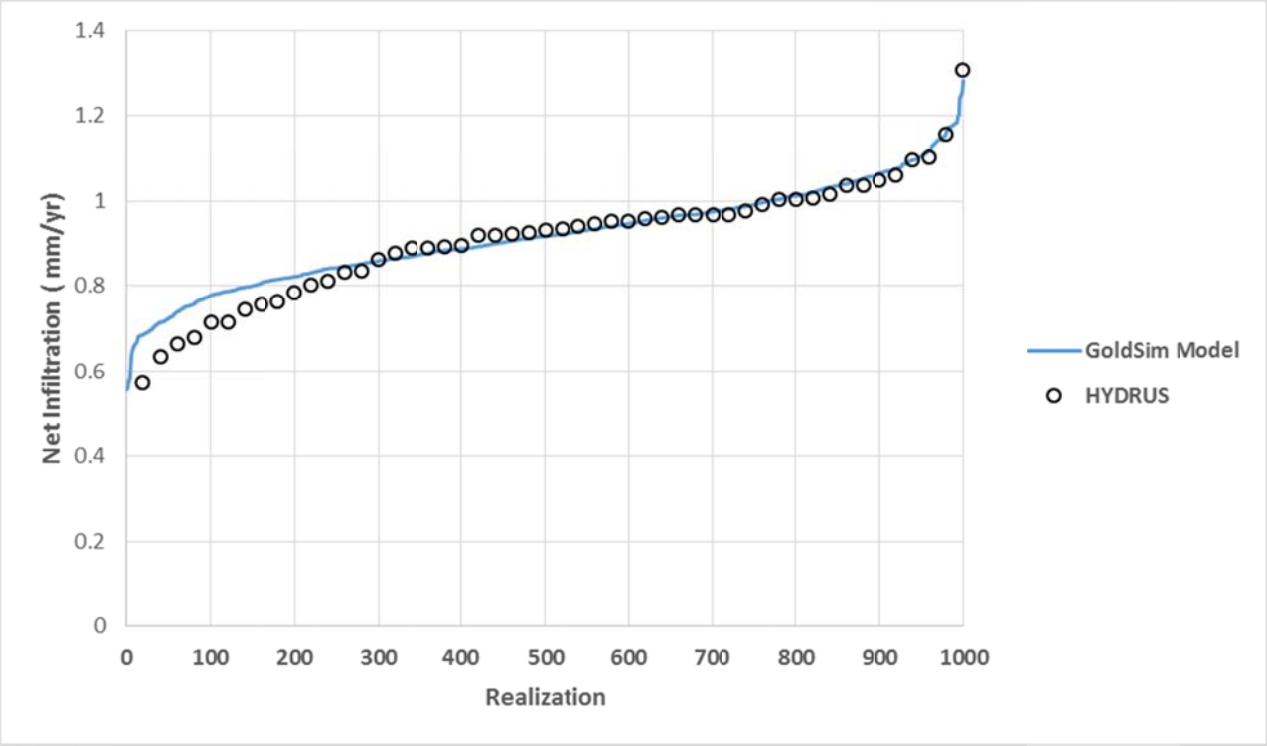

Figure 6. Comparison of 1,000 realizations of net infiltration using the linear model in GoldSim with the results of the 50 HYDRUS simulations for the naturalized cover.

4.0 Frost Damage

The infiltration modeling described in Section 2.0 takes into account the asserted "substantial disruption of near-surface layers above and within the radon barriers by frost." Hydraulic parameters used for the infiltration modeling were derived from the distributions and methods described by Dr. Craig Benson in Volume 2, Appendix E, of the SER prepared by SC&A (SC&A 2015) that represent changes in hydraulic behavior of cover materials to a naturalized state following construction. These changes are characterized by increasing values of hydraulic properties such as Ks and the hydraulic function alpha parameter that begin soon after cover completion and are commonly attributed to pedogenic processes including frost penetration. Changes in hydraulic properties of the cover used to develop the infiltration distributions for the GoldSim v1.4XXX Benson Model include homogeneous hydraulic properties (except for gravel correction of saturated water content in the surface layer), increased saturated hydraulic conductivity values, and correlation of the hydraulic conductivity and alpha hydraulic parameters to account for effects of frost damage on net infiltration rates.

5.0 Effect of Biotic Activity

The SER (SC&A 2015) describes concerns with increased flow and transport in the cover system due to biotic activity. The report comments that: "Biointrusion by plant roots can also damage cover systems, increase infiltration, and hasten migration of contaminants by increasing the hydraulic conductivity of cover-system soils penetrated by roots. This can be especially

problematic at clay radon barriers." The comment continues with references to a wide range of reported rooting depths for woody plants at Clive, from a variety of studies and literature references. The comment notes that the Utah Radioactive Material License - Condition 35 (RML UT2300249) Compliance Report (Revision 2) of July 8, 2014, submitted with the performance assessment, cites maximum rooting depth for woody plants at Clive Site of 1.3 to 2.3 ft. The comment further notes that information presented in Envirocare (2000) and Hoven et al. (2000) indicates site-specific rooting depths for greasewood of 13 ft, and that observations by DRC staff in the past have suggested that plant roots observed in borrow pits at Clive extend 10 or more feet below ground surface. These last two references are used to refute the shallow site rooting depths reported in SWCA (2013) and the Compliance Report. The comment then cites Waugh and Smith (1998) as evidence that roots can penetrate the compact clay radon barrier that occurs at 3 ft bgs in the Clive cover. Though we could not readily obtain the Waugh and Smith (1998) reference cited by the reviewer, the same information is presented in Waugh et al. (1999). Roots that penetrate the radon barrier can provide preferential pathways for infiltration.

It is important to recognize how the range of rooting depths discussed in the comment actually relates to what was used as a maximum rooting depth in GoldSim Models v1.2 and v1.4. A maximum root depth of 5.7 meters (18.7 ft) (Robertson 1983) is used in the Model, so the Model already assumes that roots extend beyond the radon barrier. In addition, v1.4 of the GoldSim Model assumes increased permeability, correlation between saturated hydraulic conductivity and the hydraulic function alpha parameter, and homogenization of the cover materials, with no physical barriers to either plant roots or infiltration.

Greasewood has been reported to extend taproots up to ~60 ft to reach groundwater (Meinzer 1927). This is not likely to occur on the Clive disposal cells, where the distance from the top of the cover to groundwater is greater than 65 ft. With groundwater beyond the reach of the taproot, the functional rooting depth of greasewood will be much shallower, and the growth of the greasewood plants will be controlled by precipitation infiltration in the upper soil horizon (Branson et al. 1976). The zone of infiltration at the site does not extend to groundwater; therefore, the use of a 60 ft maximum rooting depth is not warranted for the Clive GoldSim Model. The use of a 5.7 m maximum rooting depth is appropriately conservative because it allows for root penetration of the entire cover system, including the radon barrier, and v1.4 of the GoldSim Model assumes a naturalized cover for purposes of modeling infiltration of the cover. Note that this naturalized cover is different from the Benson homogenized cover described in Section 2.0.

6.0 Erosion

The SER (SC&A 2015) describes issues with erosion modeling documentation as unclear and a need for demonstrating the simplification of erosion modeling processes in the Clive DU PA Model. Updates were made to *Erosion Modeling for the Clive DU PA Model* (Appendix 10 of the *Final Report for the Clive DU PA Model*) based on clarification requested in Section 4.4.2 of the SER (SC&A 2015). Appendix 10 includes a detailed description of the conceptual erosion model and its implementation in the Clive DU PA Model. To assess the effects of erosion of the cover an additional model scenario was developed constructed based on the v1.4XXX Benson model described in Section 2.0. This model named "v1.4XXX Benson Erosion" includes

consideration of the receptor doses which would result from widespread erosion of the cover, as well as changes in infiltration resulting from cover erosion, described in Sections 6.1 and 6.2.

6.1 Influence of Cover Erosion on Net Infiltration

The conceptual model of cover "naturalization" described in Appendix E of the SER (SC&A 2015) is that plant and animal activity and freeze-thaw cycles result in disturbance and mixing of soil layers in the upper portion of the cover system subject to their influences. The extent of the influence of these processes decreases with depth of roots, animal burrowing, and frost penetration. This conceptual model does not maintain the designed functions of store and release layers and barrier layers to reduce net infiltration. Using this conceptual model, the upper portion of the soil profile subject to naturalization processes is considered to be homogeneous with respect to the hydraulic properties affecting net infiltration. For the Clive Site, the hydraulic properties of the waste below the cover are modeled as Unit 3 material and would be subject to the same naturalization processes as the materials used to construct the cover.

With this conceptual model, the depth to the waste would be reduced by erosion but the net infiltration will not vary. The net infiltration is determined by climate and hydraulic properties. If the hydraulic properties are assumed to be homogeneous and determined by climate and biotic activity, loss of material from the surface of the cover will not change the net infiltration.

A series of HYDRUS simulations were completed to demonstrate this concept. Input parameters for infiltration models representing two states of erosion loss were derived from the distributions and methods described by Dr. Craig Benson in Volume 2, Appendix E, of the safety evaluation report (SER) prepared by SC&A (SC&A 2015). Fifty realizations of parameters were generated and three, representing the lowest, mid-range, and highest net infiltration rates, were selected for the models. The two eroded cases chosen from the SIBERIA Model output had a loss of 6 inches (15.2 cm) of cover consisting of the surface layer, and a loss of 4 feet (122 cm) of cover corresponding to the surface layer, ET layer, frost protection layer, and the upper radon barrier. These two erosion depths were chosen based on SIBERIA Model output. SIBERIA Model results showed that 75% of the cap area has gullies that ended at 6 inches or shallower. Similarly, the results showed that 98% of the cap area has gullies that ended at 4 feet or shallower. These depths are good depth representations to explore erosion behavior.

An assumption of the one-dimensional HYDRUS model is that ponding does not occur in any channels that have been formed on the cover. Infiltration in a channel is subject to the same surface boundary condition as non-eroded portions of the cover. Given the assumptions that the hydraulic properties of the cover are homogeneous and that there is no focusing of infiltration in channels, root water uptake below channels will also be the same as in the cover outside the channel, as there will be no variation in material properties that would affect root extension or moisture distribution. All cases used 1,000-year durations for the simulations, approaching steady state. Net infiltration rates were calculated as the mean of daily simulated values from the last 100 years of the 1,000-year simulations. These results are compared with net infiltration rates from previous simulations of non-eroded covers using the same uniform hydraulic properties. For a given set of hydraulic properties, net infiltration rates are independent of the cover thickness. Small differences between the eroded and non-eroded cases are due to numerical grid differences in the non-eroded models.

Table 8. Comparison of net infiltration for eroded and non-eroded cases, for three sets of hydraulic properties.

Erosion Depth (cm)	Net Infiltration from Hydraulic Properties Set	Net Infiltration (mm/yr)
0	High	1.1
15.2	High	1.02
122	High	1.02
0	Mid-Range	0.77
15.2	Mid-Range	0.73
122	Mid-Range	0.73
0	Low	0.47
15.2	Low	0.44
122	Low	0.44

With this conceptual model of soil naturalization and the representation of waste as Unit 3 material, as soil is lost due to erosion, disturbance due to biotic activity and freeze-thaw extend to maintain the same thickness of "naturalized" soil characterized by the same ranges of hydraulic properties and thus there is no variation in the net infiltration.

6.2 Influence of Cover Erosion on Contaminant Transport and Receptor Dose

An additional model scenario was constructed to assess the effects of side-wide erosion. For this scenario, the gully formation model described in Appendix 10 was not used; instead, the entire cover was assumed to be eroded by a fixed depth throughout the simulation to assess how a thinner cover affects contaminant transport and the resulting receptor doses. Assuming the entire cover erodes produces a bounding case on the effects of erosion on risk. This erosion model is referred to as v1.4XXX Benson Erosion, and was built starting with v1.4XXX Benson. As such, this scenario assumes the homogenized parameters for the cover layers described in Section 2.6.

6.2.1 Implementation in GoldSim

The cover cell thicknesses in v1.4XXX Benson were reduced to arrive at v1.4XXX Benson Erosion. Two simulations were modeled: one in which the total cover thickness is reduced by 6 inches, and another where the cover thickness was reduced by 4 feet. Each cover cell thickness, except the top cell which remains at 1 cm, was reduced by a fixed fraction which resulted in the desired cover thickness. As the original cover was 5 feet thick, the resulting cover thicknesses in these simulations were 4.5 feet (6 inches of erosion) and 1 foot (4 feet of erosion). Plant root and animal burrowing depths were extended deeper into the cell column to account for the thinner cover. A switch is used to choose between the two erosion depths.

6.2.2 Results

Results for v1.4XXX Benson Erosion are provided in Table 9, where "6 in" and "4 ft" indicate the erosion depth. Results comparing the v1.4XXX Benson model to the erosion models indicate that downward migration of contaminants to the water table is not affected by erosion of the cover layer. This makes sense because net infiltration is not appreciably influenced by cover thickness as demonstrated in Section 6.1. Doses to the rancher receptor are increased due to a thinner amount of material above the DU waste. The thinner cover results in increased radon flux at the surface. The scenario with 4 feet of erosion showed a larger increase, as expected. However, even 4 feet of erosion across the entire cover produced less than an order of magnitudes increase, and the 95th percentile doses still remain less than 0.5 mrem/year. These results demonstrate that while receptor doses do increase with an eroded cover, doses still remain low despite the assumption of site-wide erosion of the cover.

6.2.3 Sensitivity Analysis

Sensitive parameters for v1.4XXX Benson Erosion are presented in Table 10. The sensitive parameters are the same as for v1.4 XXX Benson as described in Section 2.8.

6.2.4 Discussion

The subject modifications to the cover erosion model do not appreciably affect endpoint contaminant transport and dose. Changes to the erosion model do not need to be made to the Clive DU PA Model v1.4.

Table 9. Model results for v1.4XXX Benson Erosion.

	Mean			Median			95th Percentile		
	v1.4XXX Benson	v1.4XXX Benson Erosion		v1.4XXX Benson	v1.4XXX Benson Erosion		v1.4XXX Benson	v1.4XXX Benson Erosion	
		6 in	4 ft		6 in	4 ft		6 in	4 ft
Peak Tc-99 groundwater concentration within 500 yr (pCi/L)	7.6E3	7.6E3	7.6E3	3.0E2	3.0E2	3.0E2	4.1E4	4.1E4	4.1E4
Peak rancher dose within 10,000 yr (mrem/yr)	5.1E-2	5.7E-2	1.2E-1	4.5E-2	5.0E-2	1.0E-1	1.2E-1	1.4E-1	2.8E-1
* v1.4 results are based on 10,000 realizations, while other results in this table are based on 1,000 realizations.									

Table 10. Sensitive input parameters for v1.4XXX Benson Erosion.

	SI rank	Input parameter	Sensitivity index (SI)
Peak ^{99}Tc groundwater concentration within 500 years	1	K_d for Tc [1]	43
	2	Activity Concentration of Tc-99 in SRS DU Waste	16
	3	Molecular Diffusivity in Water	14
	4	Van Genuchten's n	5
Peak rancher dose within 10,000 years	1	Radon Escape/Production Ratio for Waste	38
	2	K_d for Ra in sand	4

[1] For technetium, the same K_d value was used for all materials.

7.0 Clay Liner

The SER (SC&A 2015) describes concern with the modeling of water flow through the clay liner below the waste in the DU PA GoldSim Model. The problems stated are:

- Flow modeling does not include a correlation between the hydraulic function parameters α and Ks.
- Flow modeling does not account for "naturalization" of the cover, which will change hydraulic function parameters.

The GoldSim software platform cannot directly model flow. A water flow rate is assigned in the GoldSim cell network for every realization based on simulations using a variably saturated flow model that is run external to GoldSim. The development of linear models for water content and net infiltration (flow rate) is described in Section 2.0 above. Net infiltration values for the entire unsaturated portion of the model were calculated using a flow model. These flow model net infiltration results were based on hydraulic function parameters for homogenized materials using the method provided in Appendix E, Volume 2, of the SER (SC&A 2015). This included use of the "Hyd Props Calculator.xls" for generating 50 hydraulic parameter sets for the HYDRUS simulations, where the values of ln(α) and ln(Ks) were correlated with a correlation coefficient of 0.48 provided in SC&A (2015). The net infiltration rate through the clay liner used for a realization of the DU PA Model represents behavior that accounts for homogenization of materials and correlation of the lnα and ln(Ks) parameters. The flow rate of water through the unsaturated cells of the GoldSim model is the same in the clay liner as it is in the radon barriers, so the above concerns are addressed through using this modeling approach.

An addition GoldSim simulation was created to assess the effects of using homogenized properties for the clay liner.

7.1 GoldSim Implementation

The following changes are implemented to model v1.4XXX Benson. The resulting model iteration is referred to as v1.4XXX Benson Clay Liner.

Porosity, bulk density, and Ks for the clay liner layers were set equal to those of the naturalized cover, which are obtained from a lookup table for each realization of the model as described in Section 2.6. The model was run for 1000 realization, and the results are summarized in Section 7.2.

7.2 Results

Results from the 1.4XXX Benson Clay Liner simulation are summarized in Table 11. The v1.4XXX models produce similar results. These results indicate that changing the clay liner properties to those of the homogenized cover does not appreciably affect endpoint contaminant transport and dose.

Table 11. Model results for v1.4XXX Benson Clay Liner.

	Mean		Median		95th Percentile	
	v1.4XXX Benson	V1.4XXX Benson Clay Liner	v1.4XXX Benson	V1.4XXX Benson Clay Liner	v1.4XXX Benson	V1.4XXX Benson Clay Liner
Peak Tc-99 groundwater concentration within 500 yr (pCi/L)	7.6E3	7.9E3	3.0E2	3.0E2	4.1E4	4.2E4
Peak rancher dose within 10,000 yr (mrem/yr)	5.1E-2	5.2E-2	4.5E-2	4.5E-2	1.2E-1	1.2E-1
* These results are based on 1,000 realizations of the models.						

7.3 Sensitivity Analysis of v.1.4XXX Benson Clay Liner

Sensitive parameters for v1.4XXX Benson Erosion are presented in Table 12. The sensitive parameters are the same as those for v1.4 XXX Benson as described in Section 2.8.

Table 12. Sensitive input parameters for v1.4XXX Benson Clay Liner.

	SI rank	Input parameter	Sensitivity index (SI)
Peak ^{99}Tc groundwater concentration within 500 years	1	K_d for Tc [1]	43
	2	Activity Concentration of Tc-99 in SRS DU Waste	16
	3	Molecular Diffusivity in Water	13
	4	Van Genuchten's n	5
Peak rancher dose within 10,000 years	1	Radon Escape/Production Ratio for Waste	38
	2	K_d for Ra in sand	4

[1] For technetium, the same K_d value was used for all materials.

7.4 Discussion

Modifications to the clay liner properties do not appreciably affect endpoint contaminant transport and dose. Changes to the clay liner properties do not need to be made to the Clive DU PA Model v1.4.

8.0 Deep Time

The SER (SC&A 2015) describes issues with deep time modeling and requests model changes. Three changes are requested in the SER:

- The material above the DU waste be modeled as Unit 3 for consistency with other Model processes that characterize waste layers as Unit 3.
- The standard deviation of the eolian deposition rate be used instead of the standard error of the mean.
- The intermediate lake sedimentation rate be changed to 10 times the large lake sedimentation rate.

In the Clive DU PA Model v1.4, Unit 3 properties were used in deep time above the DU waste layers for consistency with other near time model processes. As well, the expected grain-size characteristics of intermediate lake sediments and an expected southern flux of long-shore drift sand from the Grayback Hills southward toward the Clive site share those characteristics. This model change is acceptable.

The second and third requests in the SER were modeled to demonstrate the effects of those changes on results; however, these changes are not acceptable to implement in the Clive DU PA Model v1.4. The modeling, results and discussion are provided in the following sections.

8.1 GoldSim Implementation

The following changes are implemented to model v1.4XXX Benson; the resulting model iteration is referred to as v1.4XXX Benson Deep Time.

The depth of eolian deposition layers was set as a normal distribution with a mean of 72.7 cm and the standard deviation in the distribution was changed from 5.0 cm to 16.6 cm, as discussed above. Additionally, the sedimentation rate for intermediate lakes was calculated as ten times the deep lake sedimentation rate.

The results of this simulation are presented in Section 8.2.

8.2 Results

Endpoint results for the v1.4XXX Benson Deep Time model and the v1.4XXX Benson model are presented Table 13. Sediment concentrations increase by about double with these deep time model changes due to thinner sediment thicknesses. These sediment concentrations are still quite low.

Lake concentrations do not change much with these model changes. The amount of material above grade when the first lake returns is not affected by the model changes requested for deep time. There are sufficient amounts of radionuclides in the sediments that lake concentrations are controlled by diffusion rather than by sediment concentrations. These lake concentrations are still quite low.

Table 13. Comparison of deep time results at 90,000 yr for v1.4XXX Benson Deep Time and v1.4XXX Benson models.

	25th Percentile		Median		Mean		95th Percentile	
	v1.4XXX Benson	v1.4XXX Benson Deep Time	v1.4XXX Benson	v1.4XXX Benson Deep Time	v1.4XXX Benson	v1.4XXX Benson Deep Time	v1.4XXX Benson	v1.4XXX Benson Deep Time
U-238 lake concentration (pCi/L)	1.4E-7	1.4E-7	1.3E-5	1.3E-5	3.9E-3	3.9E-3	1.5E-2	1.5E-2
Ra-226 lake concentration (pCi/L)	2.0E-4	2.0E-4	9.4E-3	9.2E-3	6.2E-2	6.1E-2	3.0E-1	2.9E-1
U-238 sediment concentration (pCi/g)	1.3E-7	2.3E-7	5.3E-6	9.5E-6	2.4E-4	4.1E-4	1.1E-3	1.9E-3
Ra-226 sediment concentration (pCi/g)	1.7E-6	2.8E-6	7.1E-5	1.3E-4	5.8E-4	9.4E-4	2.9E-3	4.6E-3

Peak radon flux averages in deep time are 18 pCi/m^{2}s for the Clive DU PA Model v1.4 with an associated rancher dose of 0.14 mrem/yr. For v1.4XXX Benson Deep Time model they increase to 160 pCi/m^{2}s, with an associated rancher dose of 2 mrem/yr. This dose is still in an acceptable value for protection of human health.

The deep time model changes requested in the SER (SC&A, 2015) for eolian deposition and intermediate lake sedimentation are overly conservative and contradict the deep time conceptual model.

8.3 Discussion

8.3.1 Eolian deposition standard error

The measured thicknesses of eolian silt in quarry walls and excavated surfaces for the Clive Disposal Site can be found in Table 14 from field research (Neptune, 2015). The mean of the deposits is 72.7 cm, and the standard deviation is 16.6 cm. There are 11 data points, and the data are reasonably symmetric about the mean. Consequently, a normal distribution is specified for the Deep Time Model with a mean of 72.7 cm and a standard error of 5.0 cm. A reasonable simulation range considering ± 3 standard errors would be 57.5 to 87.5 cm. The minimum of the normal distribution was set to a very small number and the maximum was set to a very large number, so that the distribution was not unnecessarily restricted.

Table 14. Thickness measurements from field studies of eolian silt near Clive

Neptune Field Studies December 2014				
Site	**GPS Coord** UTM E	**GPS Coord** UTM N	**Silt Thick** (cm)	**Date** (mm/dd/yy)
Clive 29-1	321354	4508262	90.0	12/16/14
Clive 29-2	321390	4508256	80.0	12/16/14
Clive 29-3	321423	4508248	80.0	12/16/14
Clive 29-4	321502	4508236	60.0	12/16/14
Clive 29-5	321239	4508283	110.0	12/16/14
Clive 5-1	320813	4504729	55.0	12/16/14
Clive 5-2	320869	4504730	70.0	12/16/14
Clive 5-3	320914	4504731	60.0	12/16/14
Clive 5-4	321041	4504732	70.0	12/16/14
Clive Hand-Dug-1	322093	4507482	70.0	12/17/14
Clilve hand-Dug-2	320445	4507035	55.0	12/17/14
		Mean	**72.7**	
		Std Dev.	**16.6**	

This distribution represents spatio-temporal scaling, so that the distribution is of the average depth of eolian deposition at the Clive site since Lake Bonneville regressed below the site. This provides the best representation of the future eolian depositional rates over the long time frames and spatial scales of the Deep Time Model.

8.3.2 Intermediate lake sedimentation rates

The intermediate lake sedimentation rate used in the v1.4XXX Benson Deep Time model is set at 10 times the large lake sedimentation rate per review guidance. However, the assignment of a sedimentation rate for intermediate lakes derived from a deep lake sedimentation rate is not conceptually valid. The explanation for this conclusion requires re-examination of the definitions of shallow, intermediate, and deep lakes used in the *Deep Time Assessment for the Clive DU PA* white paper.

Deep lakes in the cyclical, climate driven Deep Time Assessment are similar to the Lake Bonneville stage where the dominant mode of sedimentation is deposition of carbonate (for example, the marl sedimentary facies of the Bonneville and Provo lakes). These carbonate sedimentation rates are dependent on rates of precipitation of chemical sediment (inorganic materials precipitated from the lake) and biogenic sediment (fossil remains of former living organisms). In order to form carbonate-dominated lake sediments with subordinate clastic sedimentary deposits, the elevation of a deep lake must be sufficiently higher than the elevation of the Clive site (lake depth above the site) to exclude sedimentation associated with shoreline processes and/or wave activity.

Intermediate lakes are transitory features that, by definition, reach the elevation of the Clive site. The sedimentation rate for an intermediate lake is dependent on basin location, shoreline processes, wave dynamics, presence or absence of fluvial deposition and/or local sedimentary sources, basin slope, water chemistry and biological activity. Inorganic and biogenic deposition occurs during intermediate lake cycles but is secondary to clastic sedimentation. Intermediate lakes may rise and fall about the Clive elevation but they do not reach sufficient elevations (lake depth) to deposit only carbonate sediments. Dependent on local conditions, sedimentation rates of intermediate lakes can be significantly higher than carbonate depositional rates of large lakes.

Shallow lakes are equivalent to the modern Great Salt Lake and by definition do not reach the elevation of the Clive site.

The duration of intermediate lakes is difficult to establish because they are transitory, their deposits are reworked by wave activity, and they do not preserve prominent shoreline features that can be used to establish lake chronology. Because of these limitations, the intermediate lake sedimentation parameter used in the Deep Time Assessment is a sediment thickness per lake cycle where thickness data are obtained for clastic sedimentary lake sequences using lake-core data from multiple locations in the Lake Bonneville basin. The intermediate lake thickness is an average thickness obtained from composite Lake Bonneville and pre-Lake Bonneville clastic sedimentary deposits. The deep lake sedimentation rate is established from dated cycles of deep lake marl deposits from both field observations and core studies. The deep lake sediments and the intermediate lake sedimentation thickness are controlled by different processes (carbonate precipitation versus lake-shoreline processes, respectively). The intermediate lake sedimentation rate or the thickness of intermediate lake sedimentary cycles cannot be established from the sedimentation record of deep lakes.

Iterative refinement of performance assessment models is a well-established methodology for improving the quality and information content of model results. Initial models are developed and sensitivity analysis is used to identify model parameters that most strongly affect model results. These sensitive parameters are refined, usually through focused data gathering. The performance assessment model is then rerun with refined parameters and the model results are re-examined for impact on decision objectives. Iterative updates of the Clive DU PA deep time modeling have been used to improve the usefulness of model results. However, as discussed above, using an intermediate lake sedimentation rate based on large lake sedimentation rates is not conceptually valid and degrades the model results. The initial GoldSim model results demonstrated clearly the importance of the timing and characteristics of the first return of an intermediate lake to the Clive site on resulting waste/sediment concentrations. A more effective approach to model improvements for intermediate lakes would be to focus the model structure and results on the characteristic of lake sediments at the Clive site. The intermediate lake sedimentary thickness used in the deep time model is based on patterns of sedimentation in the Lake Bonneville basin and is applied to the 2.1 million year cycle of the deep time analysis. Future model improvements should shift to the timing and characteristics of the first return of an intermediate lake at the Clive site. Deposits of the transgressive phase of Lake Bonneville and clastic sedimentary sequences below the Lake Bonneville deposits can be studied to develop sedimentation patterns of intermediate lakes specific to the Clive site.

9.0 References

Benson, C.H., et al., 2011. *Engineered Covers for Waste Containment: Changes in Engineering Properties and Implications for Long-Term Performance Assessment,* NUREG/CR-7028, United States Nuclear Regulatory Commission, Washington DC, December 2011

Branson, F.A., et al., 1976. Moisture Relationships in Twelve Northern Desert Shrub Communities Near Grand Junction, Colorado, *Ecology* 57 (6) 1104–1124

Envirocare, 2000. *Application for License Amendment for Class B & C Waste,* Envirocare of Utah Inc., North Salt Lake UT, December 2000

Hoven, H.M., et al., 2000. *Assessment of Vegetative Impacts on LLRW,* prepared for Envirocare of Utah Inc., SWCA Inc. Environmental Consultants, Salt Lake City UT, November 2000

Meinzer, O.E., 1927. *Plants as Indicators of Ground Water,* Water-Supply Paper 577, United States Geological Survey, Washington DC, 1927

Meyer, P.D., et al., 1996. *Hydrologic Evaluation Methodology for Estimating Water Movement Through the Unsaturated Zone at Commercial Low-Level Radioactive Waste Disposal Sites,* NUREG/CR-6346, PNL-10843, prepared for United States Nuclear Regulatory Commission, Pacific Northwest Laboratory, Richland WA, January 1996

Neptune, 2015. *Neptune Field Studies, December, 2014, Eolian Depositional History Clive Disposal Site,* NAC-0044_R0, Neptune and Company Inc., Los Alamos NM, March 2015

Richardson, C.W., and D.A. Wright, 1984. *WGEN: A Model for Generating Daily Weather Variables,* United States Department of Agriculture, Washington DC, August 1984

Robertson, J.H., 1983. Greasewood (*Sarcobatus vermiculatus* (Hook.) Torr.), *Phytologia* 54 (5) 309–324

SC&A, 2015. *Utah Division of Radiation Control, EnergySolutions Clive LLRW Disposal Facility, License No: UT2300249; RML #UT 2300249, Condition 35 Compliance Report; Appendix A: Final Report for the Clive DU PA Model, Safety Evaluation Report, Volume 2,* SC&A, Vienna VA, April 2015

Schroeder, P.R., et al., 1994a. *The Hydrologic Evaluation of Landfill Performance (HELP) Model, Engineering Documentation for Version 3,* EPA/600/R-94/168b, United States Environmental Protection Agency, Office of Research and Development, Washington DC, 1994

Schroeder, P.R., et al., 1994b. *The Hydrologic Evaluation of Landfill Performance (HELP) Model, User's Guide for Version 3,* EPA/600/R-94/168a, United States Environmental Protection Agency, Office of Research and Development, Washington DC, September 1994

SWCA, 2013. *EnergySolutions Updated Performance Assessment—SWCA's Response to First Round DRC Interrogatories,* SWCA Environmental Consultants, September 2013

Waugh, W.J., et al., 1999. *Plant Encroachment on the Burrell, Pennsylvania, Disposal Cell: Evaluation of Long-Term Performance and Risk,* GJO–99–96–TAR, United States Department of Energy, Grand Junction CO, June 1999

Waugh, W.J., and G.M. Smith, 1998. Root Intrusion of the Burrell, Pennsylvania, Uranium Mill Tailings Cover (invited paper), *Proceedings: Long-Term Stewardship Workshop, CONF–980652*, 1998, Grand Junction CO

Appendix A HYDRUS Simulation Results

Table 15 provides the results from the 50 HYDRUS simulations using naturalized values of hydraulic function parameters. Volumetric water contents are listed for zones in the naturalized cover corresponding to depths of the surface (WC1), evaporative (WC2), frost protection (WC3), upper radon barrier (WC4), and lower radon barrier (WC5) layers and the net infiltration at the top of the waste.

Table 15. Water content and infiltration results from 50 HYDRUS simulations using naturalized (homogenous) hydraulic properties.

Replicate	WC1 [-]	WC2 [-]	WC3 [-]	WC4 [-]	WC5 [-]	Net Infiltration (mm/yr)
1	0.129	0.161	0.163	0.163	0.163	0.74
2	0.125	0.157	0.159	0.159	0.159	0.63
3	0.099	0.126	0.127	0.127	0.126	1.31
4	0.109	0.138	0.139	0.139	0.138	1.16
5	0.132	0.166	0.167	0.166	0.166	0.99
6	0.147	0.183	0.182	0.180	0.179	0.93
7	0.161	0.200	0.201	0.200	0.199	0.86
8	0.148	0.184	0.183	0.182	0.181	0.97
9	0.114	0.144	0.145	0.145	0.144	1.10
10	0.122	0.152	0.151	0.150	0.149	1.10
11	0.140	0.175	0.176	0.176	0.175	0.89
12	0.130	0.163	0.164	0.163	0.162	1.04
13	0.148	0.185	0.185	0.184	0.184	0.95
14	0.131	0.164	0.165	0.165	0.164	0.97
15	0.150	0.187	0.189	0.189	0.189	0.68
16	0.166	0.207	0.207	0.207	0.206	0.81
17	0.130	0.164	0.164	0.164	0.163	1.00
18	0.157	0.194	0.190	0.187	0.185	0.78
19	0.121	0.152	0.154	0.154	0.154	0.72

20	0.145	0.182	0.181	0.180	0.180	0.97
21	0.175	0.217	0.219	0.219	0.219	0.57
22	0.148	0.184	0.184	0.184	0.183	0.96
23	0.131	0.164	0.165	0.164	0.164	1.01
24	0.129	0.161	0.162	0.161	0.161	1.05
25	0.153	0.189	0.188	0.187	0.186	0.93
26	0.130	0.164	0.165	0.164	0.164	1.00
27	0.145	0.181	0.183	0.183	0.183	0.76
28	0.130	0.163	0.165	0.165	0.165	0.89
29	0.141	0.177	0.177	0.176	0.176	0.93
30	0.182	0.226	0.227	0.227	0.227	0.66
31	0.151	0.187	0.187	0.185	0.185	0.92
32	0.147	0.182	0.182	0.180	0.180	0.96
33	0.126	0.158	0.160	0.160	0.160	0.95
34	0.145	0.181	0.182	0.181	0.181	0.97
35	0.129	0.162	0.163	0.162	0.161	1.04
36	0.156	0.194	0.195	0.195	0.195	0.88
37	0.125	0.157	0.159	0.159	0.159	0.83
38	0.128	0.161	0.161	0.161	0.161	1.06
39	0.142	0.177	0.179	0.178	0.178	0.83
40	0.130	0.163	0.164	0.164	0.164	0.95
41	0.173	0.214	0.216	0.216	0.216	0.72
42	0.141	0.175	0.174	0.173	0.172	0.98
43	0.133	0.167	0.168	0.167	0.167	0.94
44	0.120	0.152	0.153	0.153	0.153	0.92
45	0.135	0.169	0.170	0.170	0.170	0.89

46	0.155	0.193	0.194	0.194	0.194	0.80
47	0.137	0.171	0.172	0.172	0.172	0.76
48	0.138	0.172	0.171	0.170	0.169	1.02
49	0.118	0.149	0.151	0.151	0.151	0.92
50	0.133	0.167	0.168	0.168	0.168	0.89

Appendix B Flow Model Development Plots

The following exploratory data plots show the relationship between HYDRUS model outputs and hydraulic parameter inputs for the 50 parameter sets.

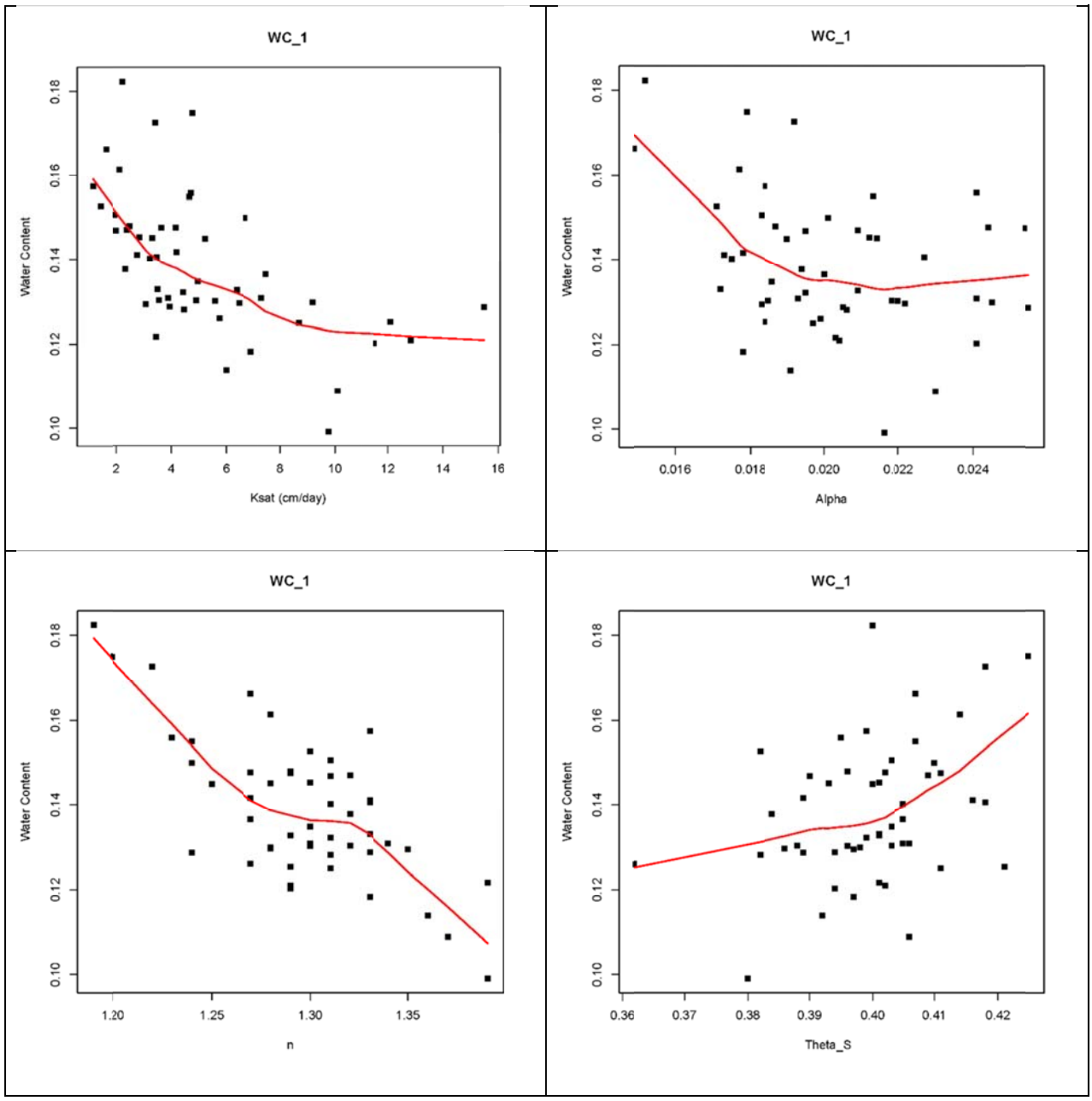

Figure 7. Relationship between model hydraulic parameters and modeled volumetric water content in the upper 6 inches of the cover.

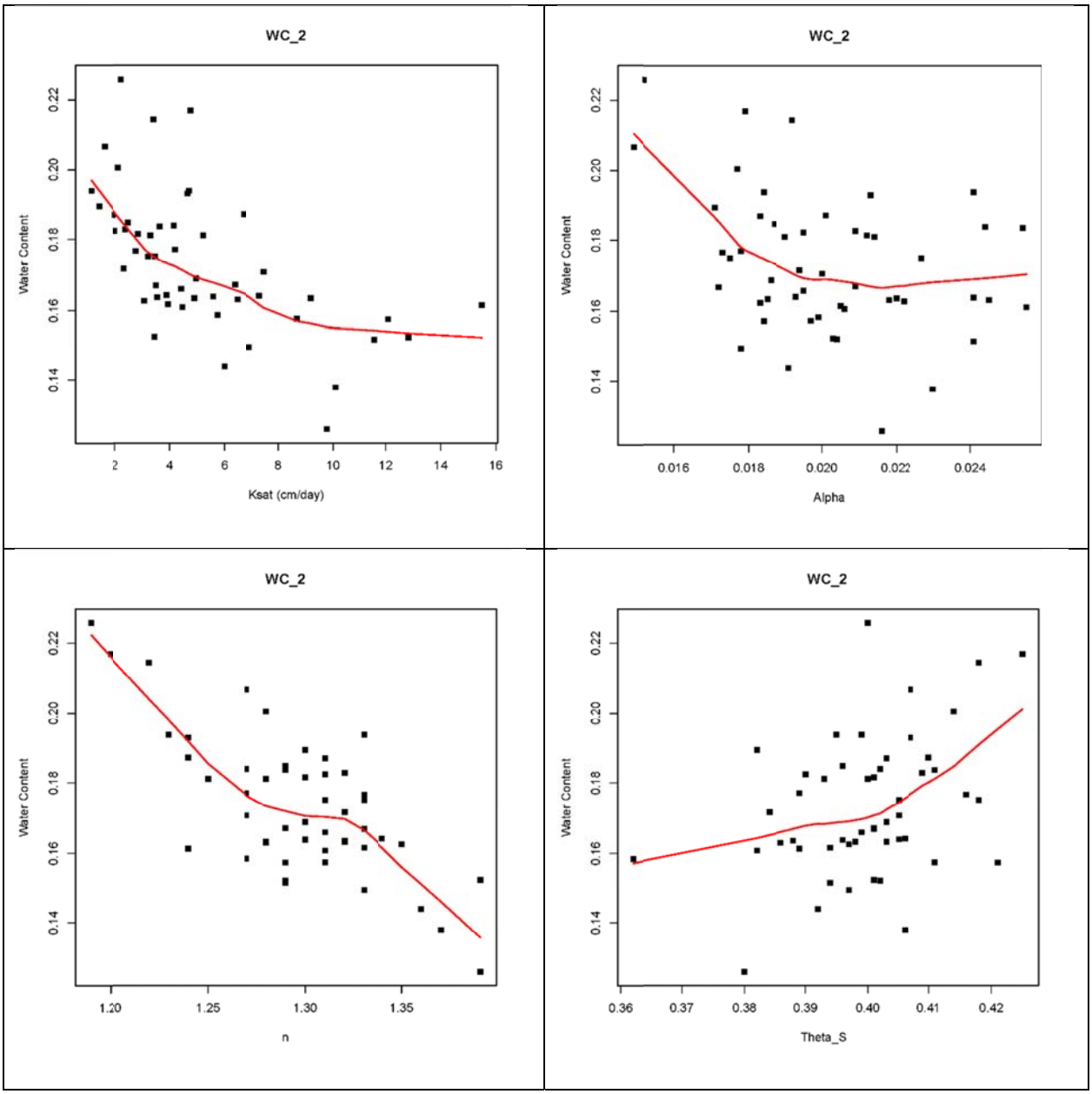

Figure 8. Relationship between model hydraulic parameters and modeled volumetric water content from 6 inches to 18 inches deep in the cover.

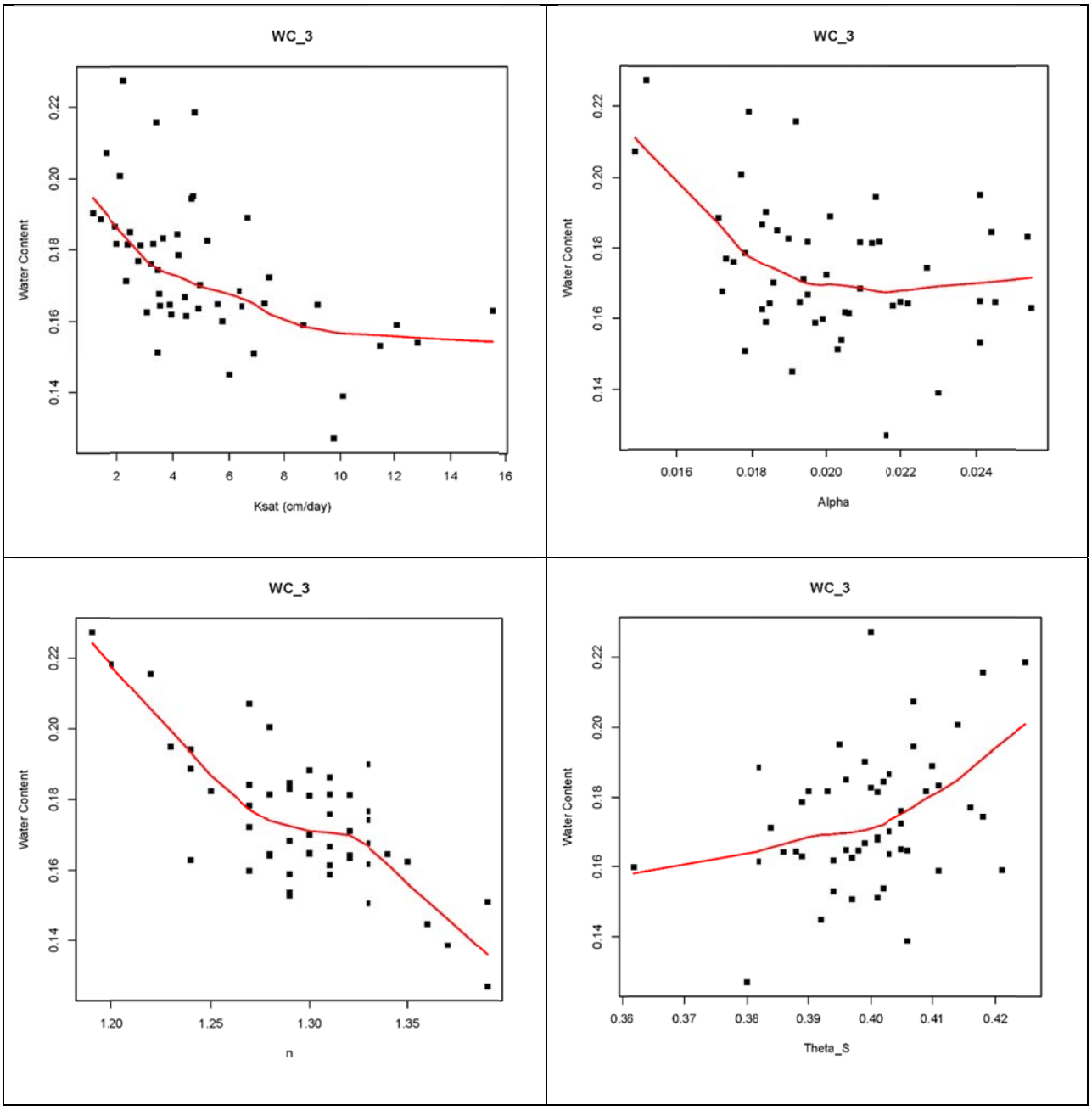

Figure 9. Relationship between model hydraulic parameters and modeled volumetric water content from 18 inches to 36 inches deep in the cover.

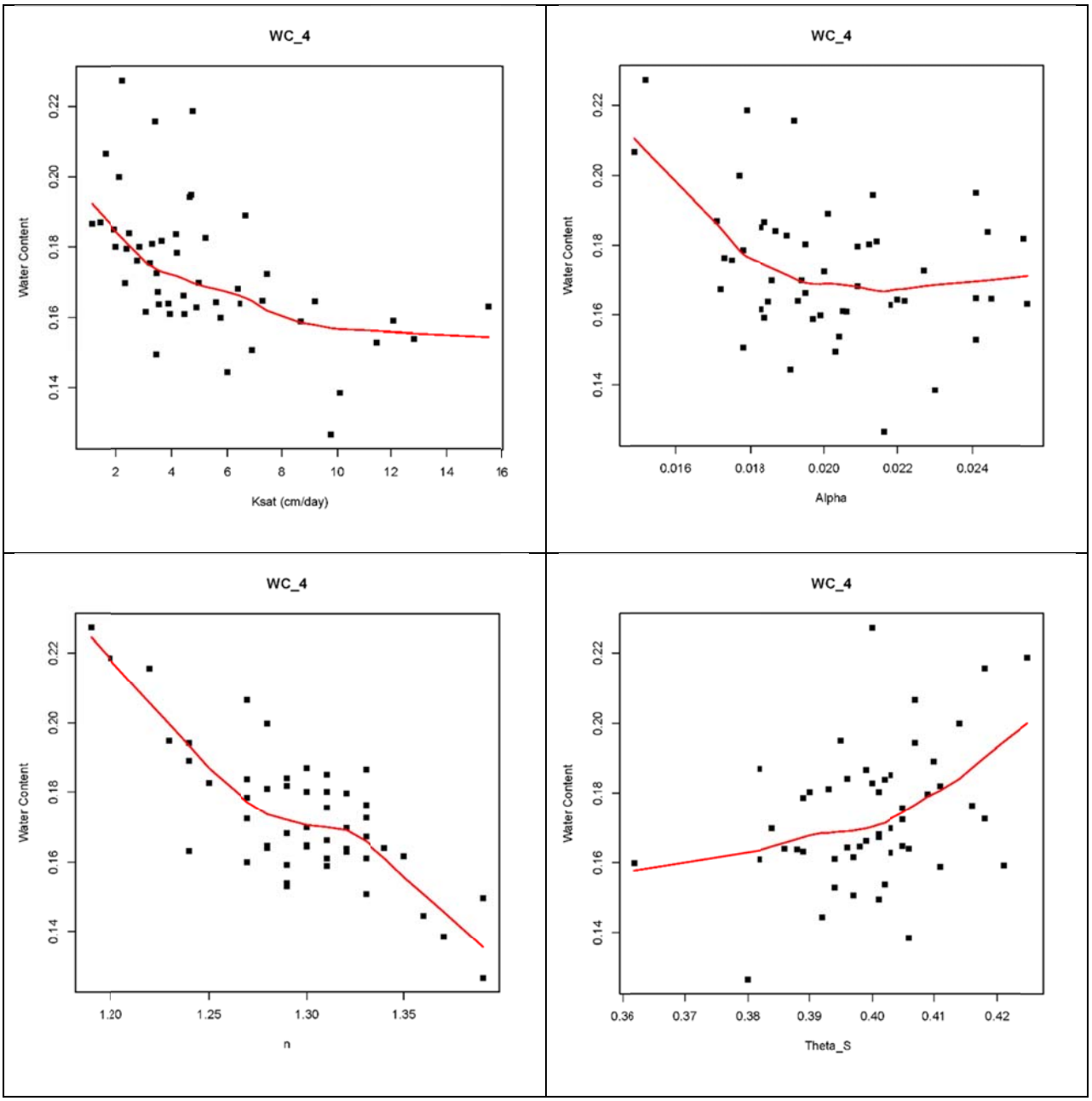

Figure 10. Relationship between model hydraulic parameters and modeled volumetric water content from 36 inches to 48 inches deep in the cover.

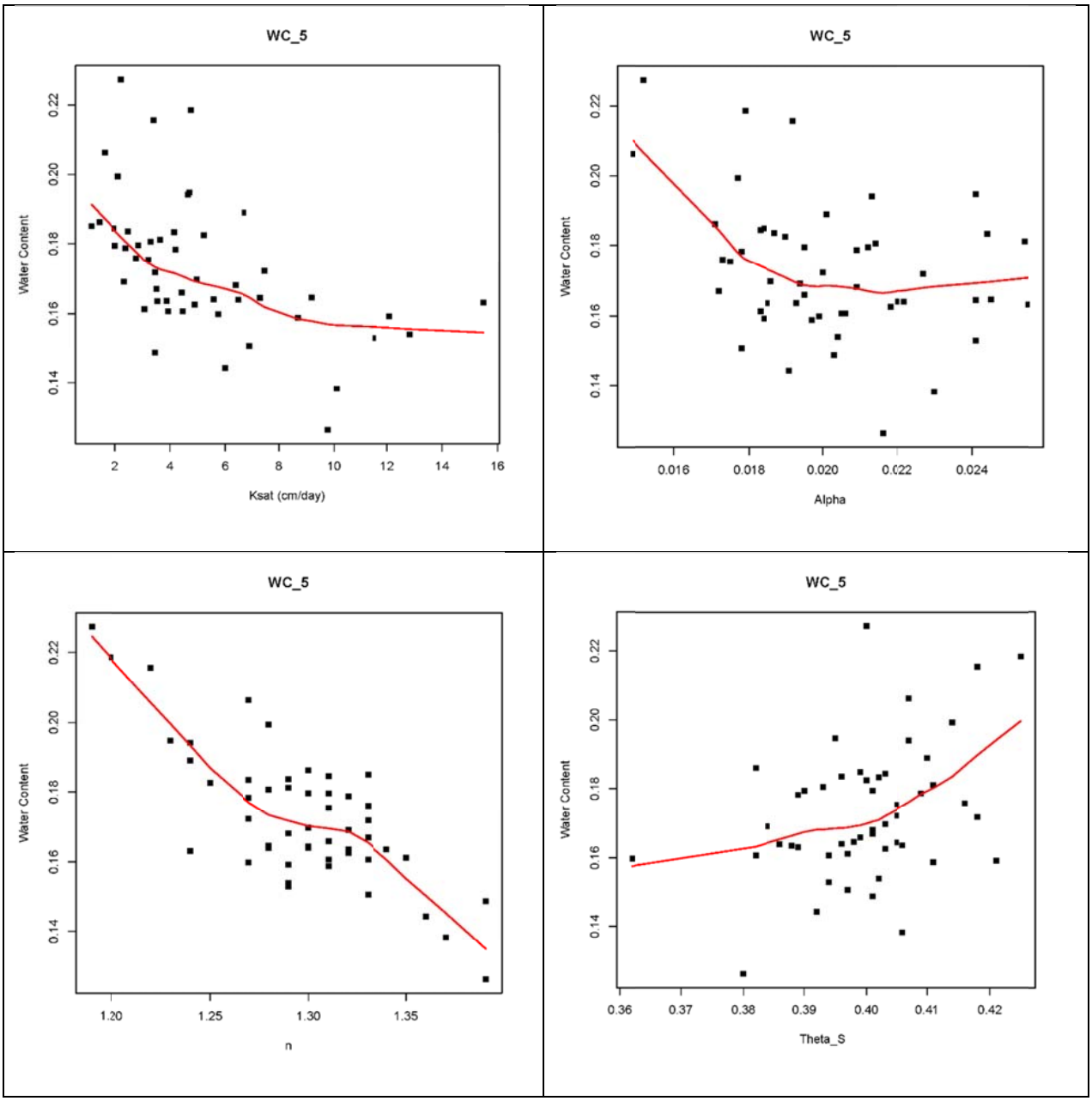

Figure 11. Relationship between model hydraulic parameters and modeled volumetric water content from 48 inches to 60 inches deep in the cover.

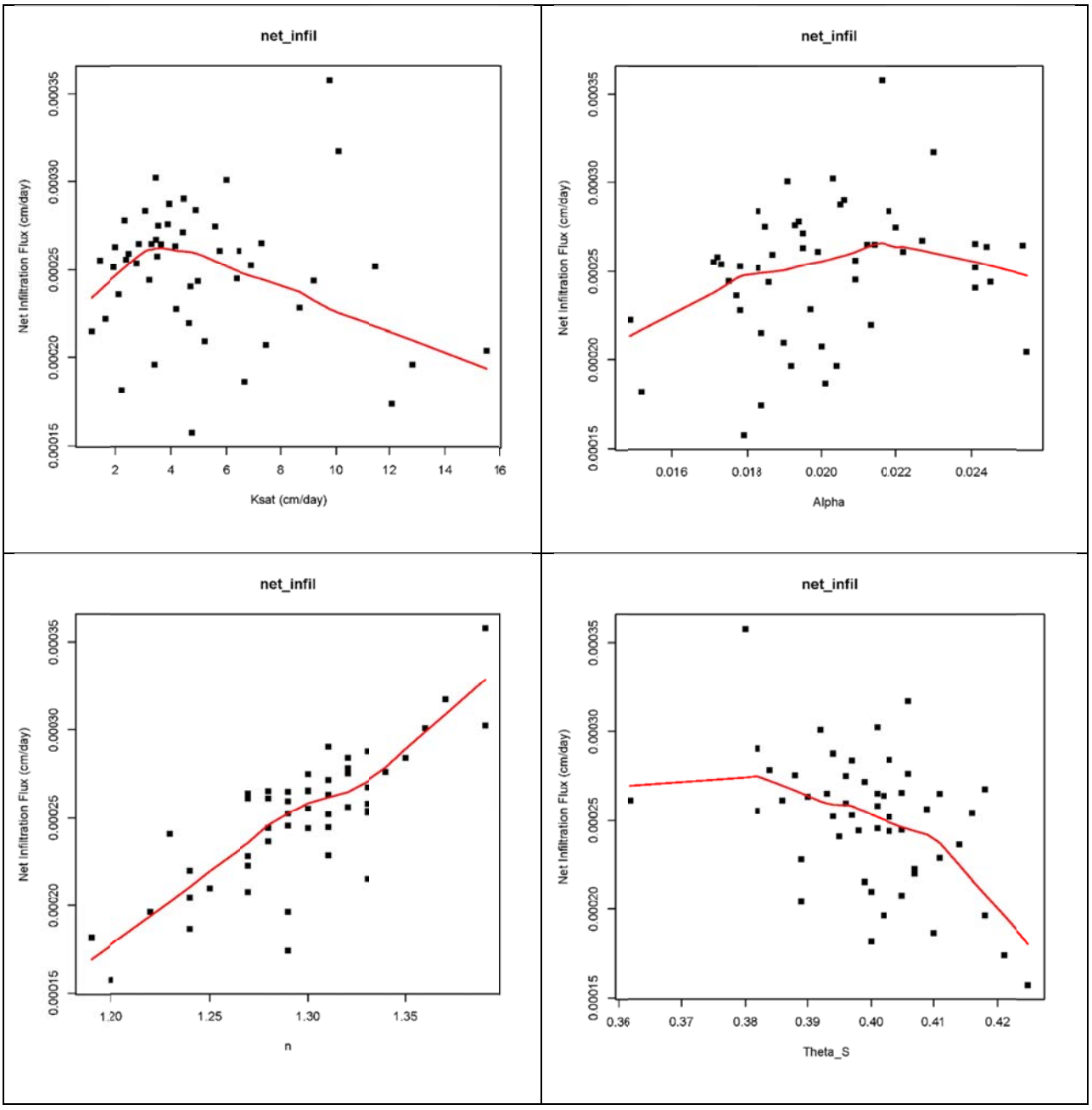

Figure 12. Relationship between model hydraulic parameters and modeled net infiltration at the the top of the waste.

The following plots show the fit between the HYDRUS model results for volumetric water content and net infiltration and the linear models built into the GoldSim v1.4XXX Benson Model for specifying water flow.

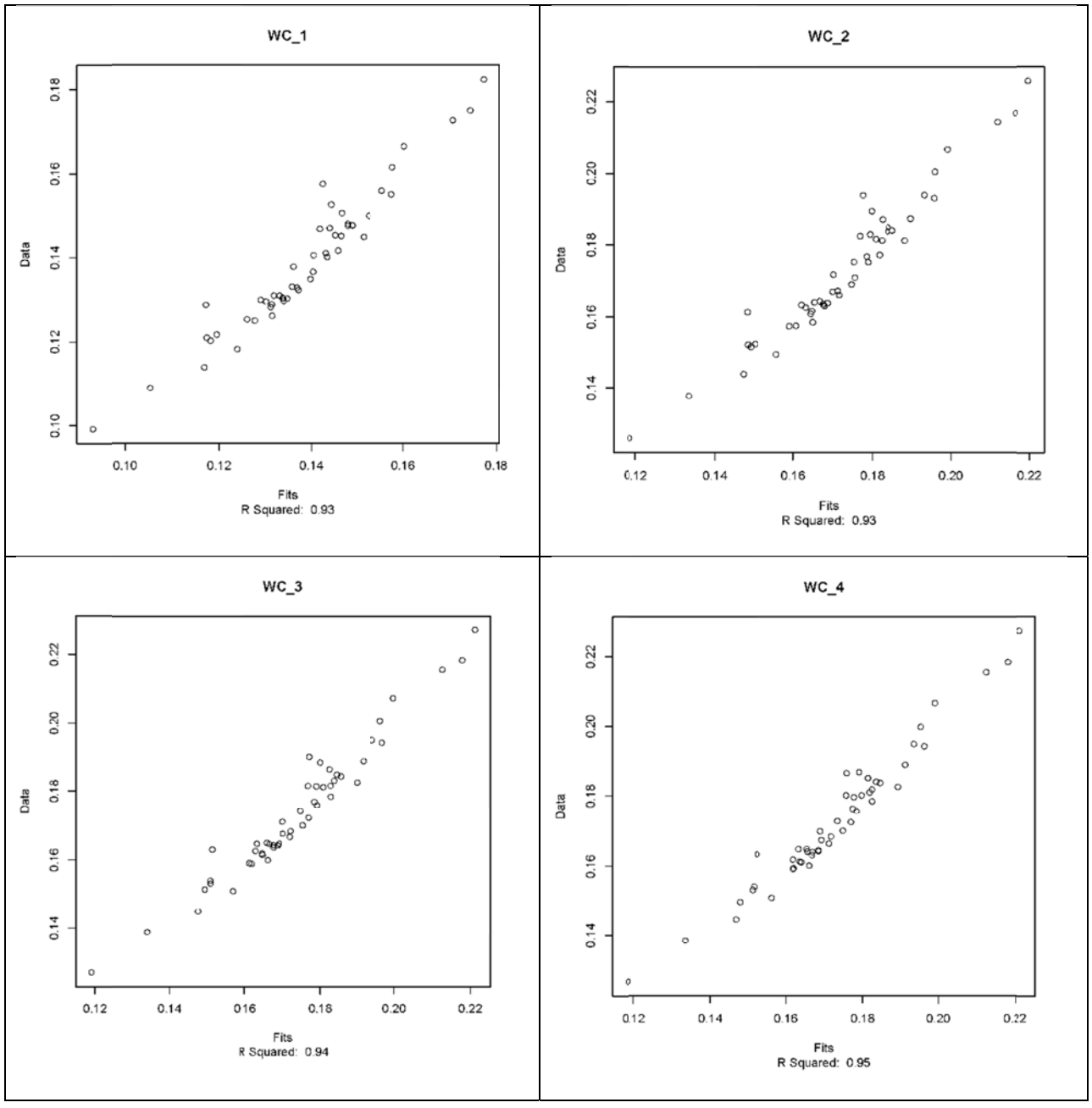

Figure 13. HYDRUS volumetric water contents plotted with linear model values for the surface through the upper radon barrier of the cover.

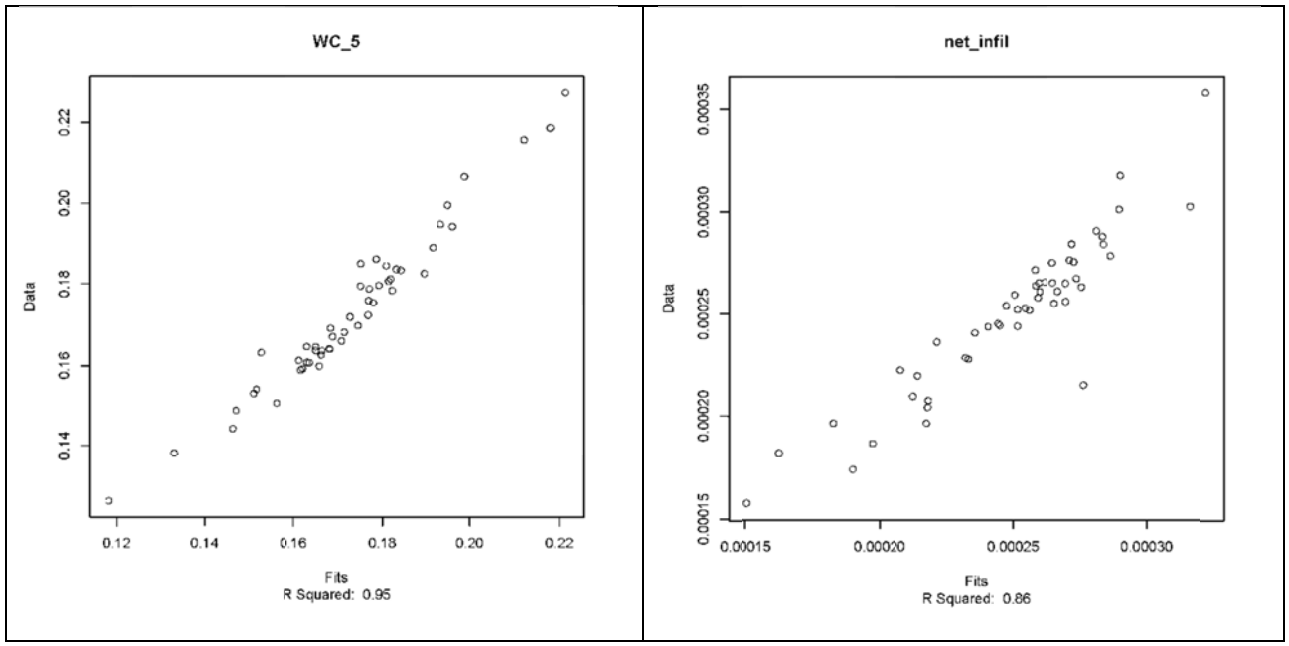

Figure 14. HYDRUS volumetric water content for the lower radon barrier and net infiltration into the top of the waste plotted with linear model values.